ELSEVIER

Journal of Non-Crystalline Solids 204 (1996) 294–300

JOURNAL OF NON-CRYSTALLINE SOLIDS

Letter to the Editor

Silicon site distributions in an alkali silicate glass derived by two-dimensional ^{29}Si nuclear magnetic resonance

P. Zhang [a], C. Dunlap [a], P. Florian [a], P.J. Grandinetti [a,*], I. Farnan [b], J.F. Stebbins [c]

[a] *Department of Chemistry, The Ohio State University, 120 W. 18th Avenue, Columbus, OH 43210-1173, USA*
[b] *Department of Earth Sciences, Cambridge University, Downing Street, Cambridge CB2 3EQ, UK*
[c] *Department of Geological and Environmental Sciences, Stanford University, Stanford, CA 94305-2115, USA*

Received 22 May 1996; revised 26 August 1996

Abstract

A common approach to quantify $Q^{(n)}$ species in silicate glasses is to use ^{29}Si magic-angle spinning (MAS) nuclear magnetic resonance (NMR) and assume that the overlapping isotropic chemical shift distributions of $Q^{(n)}$ species are Gaussian. We have shown that a two-dimensional isotropic/anisotropic ^{29}Si NMR experiment can not only determine the distributions of $Q^{(n)}$ species without any a priori assumptions about the distribution, but can also provide over an order of magnitude improvement in the precision of $Q^{(n)}$ species quantification in silicate glasses. Using this approach we have investigated an alkali silicate glass of composition $2Na_2O \cdot 3SiO_2$ and have observed a small concentration of $Q^{(4)}$ in a sample mainly having $Q^{(2)}$ and $Q^{(3)}$. We have found that the distribution of isotropic chemical shifts for each of the $Q^{(n)}$ is approximately Gaussian. The relative populations of $Q^{(2)}$, $Q^{(3)}$, and $Q^{(4)}$ obtained from these separated distributions give an equilibrium constant of 0.0129 ± 0.0001 for the disproportionation reaction $2\ Q^{(3)} \rightleftharpoons Q^{(2)} + Q^{(4)}$. This value is slightly higher than what is obtained from analyzing the one-dimensional MAS spectrum alone, thus revealing a higher degree of disorder in speciation and configurational entropy for the glass.

Researchers interested in the 'structure' of a glass often focus on measuring statistical distributions of various structural motifs on various length scales. In silicate glasses one such motif is the type of silicate tetrahedral species. There are five types of silicate tetrahedra each characterized by their connectivity, i.e., the number of oxygen that are corner-linked to other tetrahedra. These are denoted by the notation $Q^{(n)}$, where n (~ 0–4) represents the number of bridging oxygen per tetrahedron. Quantifying the distribution of $Q^{(n)}$ species in a silicate glass can provide insights into many aspects of silicate chemistry.

Solid-state ^{29}Si NMR has been used extensively to investigate alkali silicate glasses [1–7] and provided the most convincing evidence that the $Q^{(n)}$ species distribution is not random but closer to binary (i.e., contains a maximum of two $Q^{(n)}$ species, with a sequential appearance of $Q^{(n-1)}$ species as the alkali content increases). This information has been valuable in testing thermodynamic models of alkali silicate glasses [8,9]. One popular model, which in-

* Corresponding author. Tel.: +1-614 292 6818; fax: +1-614 292 1685; e-mail: grandinetti.1@osu.edu.

PII S0022-3093(96)00601-1

volves the disproportionation equilibria between $Q^{(n)}$ species,

$$2Q^{(n)} \rightleftharpoons Q^{(n-1)} + Q^{(n+1)}, \quad \text{where } n = 3, 2, 1,$$

associated with the glass transition temperature, has been used in understanding the energetics and thermodynamic mixing properties of silicate melts [10,11] and suggested as a mechanism for alkali ion transport in alkali silicate glasses [12]. Although ^{29}Si NMR and this thermodynamic model of $Q^{(n)}$ species disproportionation equilibria has been used to predict reasonable activation energies for ionic transport [12], these ^{29}Si results are based on the fitting of heavily overlapping lines, and could be severely biased by the commonly made assumption that the individual MAS NMR lineshapes are Gaussian [7,13].

In an earlier work [14] we showed how a two dimensional isotropic/anisotropic ^{17}O NMR correlation experiment can be used to separate overlapping anisotropic ^{17}O lineshapes in a $K_2Si_4O_9$ glass according to their isotropic frequencies and then used to quantify the local structural distributions around oxygen in an alkali tetrasilicate glass, in this case obtaining Si–O–Si angle distribution. This approach has been extended to other nuclei using the same or related 2D NMR techniques to investigate glass structures [15–18]. In this letter we use this approach to determine silicon site distributions independent of any assumptions about the structure of the glass and show that the precision in quantifying the $Q^{(n)}$ species distribution can be improved by over an order of magnitude compared with previous approaches.

Under static conditions or off-magic angle spinning, each $Q^{(n)}$ species exhibits an anisotropic NMR lineshape as shown in Fig. 1 due to the anisotropy (CSA) of the chemical shift interaction. This interaction arises from the magnetic shielding produced by the electron cloud surrounding the nucleus and therefore reflects the nature and directionality of the bonding. It is characterized by three parameters: isotropic position δ_{iso}, axiality Δ, and asymmetry parameter η. δ_{iso} reflects the mean silicon environment, Δ measures the extent of the electron cloud distortion and η expresses the departure from a cylindrically symmetric environment ($\eta = 0$ (symmetric) $\rightarrow$ 1 (asymmetric)). $Q^{(0)}$ and $Q^{(4)}$ sites have the smallest axiality due to their highly symmetric environment. The remaining sites have relatively large axialities, with $Q^{(3)}$ and $Q^{(1)}$ sites having low asymmetry parameters which reflect the fact that their environment is close to axial symmetry. Under MAS conditions where anisotropic broadening (i.e., information on Δ and η) is removed those five units are mainly identified only by their isotropic position, δ_{iso}, which approximately ranges from -70 ppm for $Q^{(0)}$ to -110 ppm for $Q^{(4)}$ [19] with some considerable overlap. In principle, the knowledge of all three chemical shift tensor values, δ_{iso}, Δ and η, as opposed to only δ_{iso} as measured under MAS conditions, should provide a much more reliable method of separating overlapping isotropic (MAS) line shapes.

For each type of $Q^{(n)}$ site in a glass there also exists a continuous structural distribution arising from second coordination sphere disorder such as a distribution of Si–O–Si bond angles, variations in non-bridging oxygen–alkali distances and higher coordination sphere (i.e., medium-range) disorder. This disorder results in a distribution of chemical shift parameters for each type of $Q^{(n)}$ site that in turn leads to an inhomogeneous broadening of each $Q^{(n)}$ resonance in the MAS and static NMR spectra. In order to quantify the relative $Q^{(n)}$ species populations in silicate glasses using one-dimensional (1D) MAS a least-squares analysis of the MAS lineshape is performed with the common assumption that the MAS lineshape is a superposition of Gaussian lineshapes, one for each $Q^{(n)}$ species present. Unfortunately, strong overlap of $Q^{(n)}$ resonances in the MAS spectra leads to large covariances between best fit intensity parameters and this results in significant uncertainties in the relative populations of $Q^{(n)}$ species. By exploiting the high symmetry of the $Q^{(4)}$ site, 1D static ^{29}Si NMR experiments [2,4] have been used to improve the precision of $Q^{(4)}$ quantification. However, assumptions about the $Q^{(n)}$ lineshapes are still required and relatively large covariances between best fit intensity parameters still exist. The separation of anisotropic lineshapes obtained in a two-dimensional isotropic/anisotropic NMR spectrum provides a means of determining the distributions of $Q^{(n)}$ species without any a priori assumptions about the distribution and also significantly reduces the covariances between best fit parameters and thus increasing the precision of the site populations.

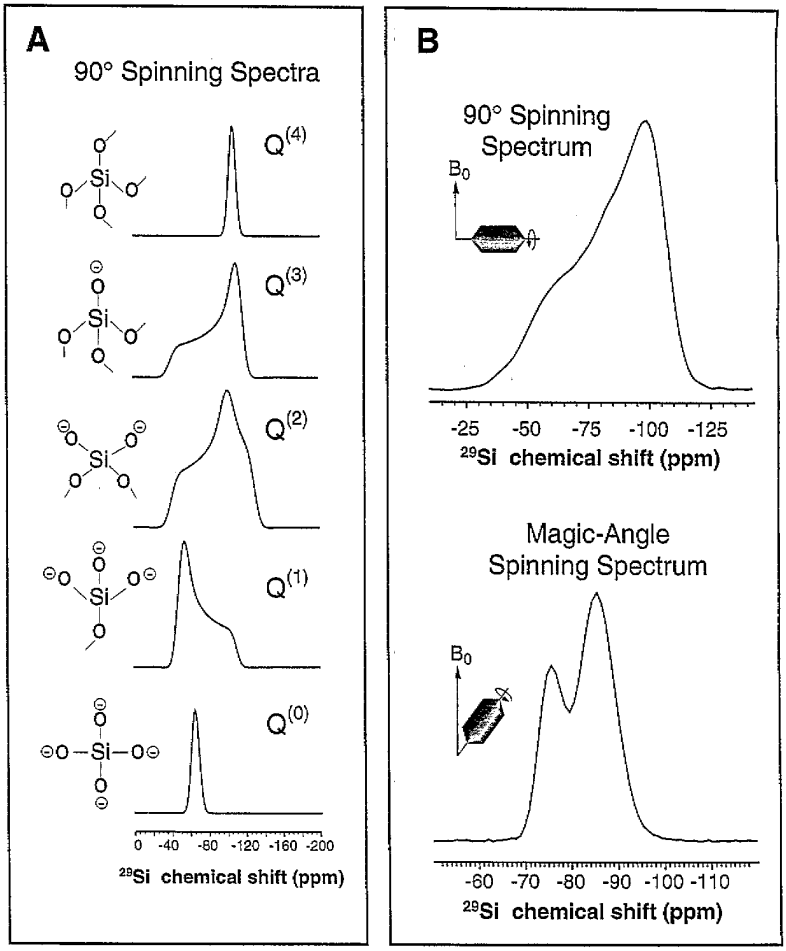

Fig. 1. (A) One-dimensional ^{29}Si anisotropic (90° spinning) NMR lineshapes for the five different silicate tetrahedral environments in silicate glasses. Lineshape parameters are based on typical values found in crystalline compounds. (B) On top is the one-dimensional ^{29}Si anisotropic (90° spinning) NMR lineshape and on bottom is the one-dimensional ^{29}Si MAS (54.74° spinning) NMR lineshape for $2Na_2O \cdot 3SiO_2$ glass. The vertical axes (not shown) are intensity in arbitrary units.

There are numerous ways to obtain a two-dimensional (2D) isotropic/anisotropic correlation spectrum [20–24]. We have adopted a modified approach [25] based on the sequence of Bax et al. [20], where the NMR spectrum while spinning at the magic angle is correlated with that while spinning at an axis perpendicular to the magnetic field. When spinning perpendicular to the magnetic field the static sample anisotropic lineshapes are scaled [26] by a factor of -0.5 as shown in Fig. 1. We have chosen a sodium silicate glass sample [27] [1] of composition $2Na_2O \cdot 3SiO_2$ enriched to 95% in ^{29}Si. This composition is expected to contain both $Q^{(2)}$ and $Q^{(3)}$ type sites. It is

[1] The sample was synthesized from high purity Na_2CO_3 and 95% ^{29}Si enriched SiO_2 (Oak Ridge Laboratory), with 0.2 wt% Gd_2O_3 added to enhance spin–lattice relaxation. The starting mixture was decarbonated overnight at 770°C. The weight loss during synthesis was within 0.1% absolute of nominal.

well established that deviations from a binary distribution will also result in the presence of $Q^{(4)}$ sites.

A stacked plot of the ^{29}Si 2D (90°, 54.74°) correlation spectrum of $2Na_2O \cdot 3SiO_2$ glass is shown in Fig. 2(A). A contour plot along with representative cross-sections and best-fit simulations is shown in Fig. 2(B). Recalling the characteristic anisotropic lineshapes shown in Fig. 1 it is clear from the 90° dimension that the low intensities of the MAS lineshape near −100 ppm are dominated by $Q^{(4)}$, the

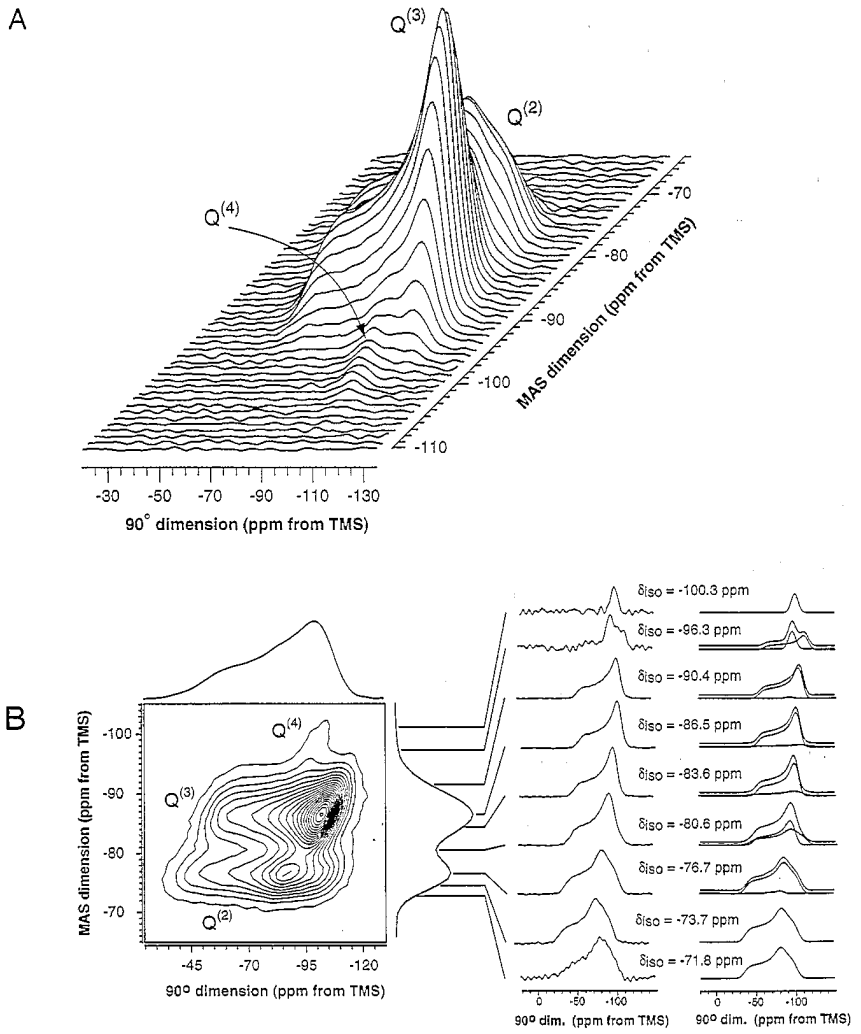

Fig. 2. (A) Stacked plot of two-dimensional ^{29}Si isotropic/anisotropic correlation spectrum. The experiment was performed on a Chemagnetics 9.4 T (79.48 MHz for ^{29}Si) NMR spectrometer using a modified version of a home-built DAS probe described earlier [28]. The experiment was done at ambient temperature with sample spinning rate of 11.6 kHz. ^{29}Si relaxation time was measured using inversion recovery experiment under MAS condition and T_1 for both $Q^{(2)}$ and $Q^{(3)}$ were found to be 10 s. A pulse delay of 25 s was chosen. The angle pair (54.74° and 90°) was employed with detection made at 54.74°. $\pi/2$ times were chosen to be 4.3 μs at 54.74° and 4.0 μs at 90°. The number of scans was 128, the number of $t_1 \times t_2$ points are 77×512, with dwell time of 50 μs and 25 μs, respectively. (B) Contour plot with projection on each dimension. 20 equally spaced contour lines are drawn at levels ranging from 3 to 93% of the maximum intensity in the spectrum. On the right are selected cross-sections and their 'best-fit' curves. 36 cross-sections from $\delta_{iso} = -71.02$ ppm to -106.16 ppm were analyzed. The average χ_ν^2 value was ~ 4 with a standard deviation of ~ 3. The vertical axes (not shown) are intensity in arbitrary units.

MAS lineshape intensities around −88 ppm are dominated by $Q^{(3)}$ and the MAS lineshape intensities around −75 ppm are dominated by $Q^{(2)}$. The chemical shift anisotropy lineshapes in the individual cross-sections taken parallel to the 90° dimension were least-squares analyzed to obtain the relative contribution of each $Q^{(n)}$ species to the MAS intensity at the MAS frequency correlated to that cross-section. Again, this approach has the advantage that the parameter uncertainties in each cross-section are completely uncorrelated with parameter uncertainties in other cross-sections. The chemical shift anisotropy lineshape for each site was modeled using five parameters. These were (1) an isotropic chemical shift position δ_{iso}, (2) a chemical shift tensor axiality Δ, (3) a chemical shift tensor asymmetry parameter η, (4) an integrated intensity and (5) a Gaussian smoothing function. All sites in each cross-section shared the same isotropic frequency and that value was fixed by the isotropic dimension. In initial least-squares analyses those cross-sections dominated by one $Q^{(n)}$ species showed little variations in Δ, η and Gaussian line broadening for the line shape of the dominant species. In cross-sections with strong overlap of $Q^{(n)}$ species and/or low signal-to-noise the least-squares analyses gave discontinuous unphysical variations in the parameters. Therefore, in performing the final least-squares analysis of each cross-section the chemical shift tensor axiality Δ and asymmetry parameter η for a given $Q^{(n)}$ site were held fixed at the values obtained when that $Q^{(n)}$ site was the dominate species in the cross-section. Thus all sites were constrained to have the same Gaussian smoothing function equivalent to 850 Hz and Δ and η were fixed at $\Delta = -78$ ppm, $\eta = 0.53$ for $Q^{(2)}$, $\Delta = -69$ ppm, $\eta = 0.03$ for $Q^{(3)}$ and $\Delta = 0.0$ ppm, $\eta = 0.0$ for $Q^{(4)}$. These results are in good qualitative agreement with previous mean chemical shift anisotropy parameters obtained by fitting the static spectrum of several sodium silicate compositions [2,4].

In Fig. 3 is the MAS spectrum obtained from the projection of the 2D spectrum onto the 54.74° axis, along with the individual component lineshapes for each of the $Q^{(n)}$ species present in the glass. The individual component lineshapes had been constructed with the integrated intensity information derived from the least-squares analyses of the anisotropic cross-sections. From these data we have found that the distribution of isotropic chemical shifts for each of the $Q^{(n)}$ resonances; in this case it appears that the distributions are approximately Gaussian. The $Q^{(4)}$ site has a Gaussian distribution as found previously for SiO_2 glass [29]. The relative concentrations we obtain for the three $Q^{(n)}$ species (± one standard deviation) are 1.59 ± 0.01%, 63.73 ± 0.06% and 34.68 ± 0.07% for $Q^{(4)}$, $Q^{(3)}$ and $Q^{(2)}$, respectively. We assume that systematic errors in our analysis are dominated by anisotropic lineshape distortions arising from intensity lost to spinning sidebands. In this case the sideband intensities are ~5% of the total intensity. We can redistribute this intensity between the $Q^{(3)}$ and $Q^{(2)}$ sites (assuming $Q^{(4)}$ sideband intensities are negligible), using the $Q^{(3)}$ and $Q^{(2)}$ percentages above (renormalized) as a first approximation. With this correction we report 1.51 ± 0.01%, 63.78 ± 0.06% and 34.71 ± 0.07% for $Q^{(4)}$, $Q^{(3)}$ and $Q^{(2)}$ respectively.

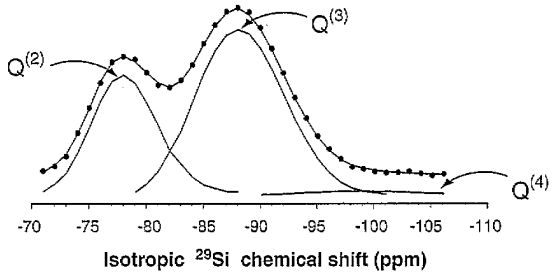

Fig. 3. The separated isotropic lineshapes for each $Q^{(n)}$. The reconstructed MAS spectrum from the sum of the three isotropic lineshapes is shown above, along with the observed MAS spectrum shown in black dots. The vertical axis (not shown) is intensity in arbitrary units.

Using these populations we can calculate for the disproportionation reaction,

$$2Q^{(3)} \rightleftharpoons Q^{(2)} + Q^{(4)}, \quad (1)$$

the equilibrium constant at the glass transition temperature,

$$K = [Q^{(4)}][Q^{(2)}]/[Q^{(3)}]^2. \quad (2)$$

For this composition we obtain $K = 0.0129 \pm 0.0001$. Our measured populations also agree with the expected Na/Si ratio of the charge balance equation:

$$4[Q^{(0)}] + 3[Q^{(1)}] + 2[Q^{(2)}] + 1[Q^{(3)}] + 0[Q^{(4)}] = \mathrm{Na/Si}. \quad (3)$$

Each $Q^{(n)}$ species has a charge of $-(4-n)$, which is balanced by the $+1$ charge of the sodium cations. From the composition the expected Na/Si ratio is 4/3. The Na/Si ratio calculated using the equation above and the relative populations we have measured is 1.332 ± 0.011. This value agrees reasonably well with the expected value and offers additional evidence that our measured populations are accurate.

It is interesting to note that the approximately Gaussian shapes that describe the distribution of the chemical shifts of each $Q^{(n)}$ species are slightly different from those that would be obtained by a least-squares analysis of the MAS projection. In a Gaussian lineshape least-squares analysis of the MAS projection only, the relative concentrations of $Q^{(n)}$ species obtained (with sideband correction) for the three $Q^{(n)}$ species are $1.6 \pm 0.7\%$, $68.2 \pm 0.7\%$ and $30.2 \pm 0.2\%$ for $Q^{(4)}$, $Q^{(3)}$ and $Q^{(2)}$ respectively. These values result in a lower K of 0.0106 ± 0.0046 in agreement with values obtained previously by fitting MAS spectra of a range of sodium silicate glass compositions [3]. While there may be slight systematic errors still unaccounted with the 2D approach, it is clear that the latter is more than an order of magnitude more precise in quantifying $Q^{(n)}$ species distributions than is fitting of 1D MAS spectra only. The value of K obtained here from the 2D spectrum is also higher than that obtained from the static 1D spectrum of $Na_2Si_2O_5$ glass [30]. The significance of this difference is not clear, given that results in this earlier study were not obtained by least-squares regression, making uncertainties difficult to estimate. However, the difference may in fact reflect a compositional dependence of the thermodynamic activity coefficients, which we have neglected in Eq. (2). Such a variation may be expected from the known non-ideality of binary Na_2O–SiO_2 solutions.

The equilibrium constant K ranges from $K = 0$ for a highly ordered (i.e., binary) configuration to $K = 0.375$ for a completely random configuration [31]. Our measured value of K is slightly higher than that obtained by analyzing the 1D MAS spectrum alone, implying a slightly more disordered mixing of bridging and non-bridging oxygen. This improvement in quantification should have a significant impact on furthering our understanding of how configurational changes impact thermodynamic and transport properties of silicate melts. Future work includes a more quantitative investigation of speciation with changing modifying cation field strength, fictive temperature and possibly pressure.

Finally, we note that the assumption of constant chemical shift anisotropy parameters (i.e., Δ and η) implies that the principle components of the chemical shift tensor, i.e., σ_{XX}, σ_{YY}, and σ_{ZZ} vary linearly with isotropic chemical shift, δ_{iso}. Recalling that

$$\begin{aligned} \sigma_{XX} &= \delta_{iso} - \tfrac{1}{2}\Delta(1-\eta), \\ \sigma_{YY} &= \delta_{iso} - \tfrac{1}{2}\Delta(1+\eta), \\ \sigma_{ZZ} &= \delta_{iso} + \Delta. \end{aligned} \tag{4}$$

This trend could be attributed to a number of structural variations such as changes in the coordination number of non-bridging oxygen, changes in the distance of the oxygen from its sodium neighbors and/or changes in the length of the Si–O bond lengths. It is clear that data on chemical shift anisotropies for silicate species in glasses, coupled with an enlarged data set for crystalline analogues and with improved theoretical treatment, could lead to a significant growth in our understanding of the nature of structural disorder. The measurement of such parameters, as well as the precision of the determination of species concentrations, has been significantly enhanced by the 2D isotropic/anisotropic correlation experiment presented here.

Acknowledgements

The authors thank Jay Baltisberger for helpful discussions. This work was supported by grants to P.J.G. from the National Science Foundation (No. CHE-9501872) and the Donors of The Petroleum Research Fund, administered by the American Chemical Society.

References

[1] R. Dupree, D. Holland, P.W. McMillan and R.F. Pettifer, J. Non-Cryst. Solids 68 (1984) 399.
[2] J.F. Stebbins, Nature 330 (1987) 465.
[3] H. Maekawa, T. Maekawa, K. Kawamura and T. Yokokawa, J. Non-Cryst. Solids 127 (1991) 53.
[4] J.F. Emerson, P.E. Stallworth and P.J. Bray, J. Non-Cryst. Solids 113 (1989) 253.

[5] A.R. Grimmer et al., Phys. Chem. Glasses 25 (1984) 105.
[6] C.M. Schramm, B.H.W.S. de Jong and V.E. Parziale, J. Am. Chem. Soc. 106 (1984) 4396.
[7] H. Eckert, Prog. Nucl. Magn. Reson. Spectrosc. 24 (1992) 159.
[8] W.G. Dorfeld, Phys. Chem. Glasses 29 (1988) 179.
[9] S.J. Gurman, J. Non-Cryst. Solids 125 (1990) 151.
[10] A. Navrotsky, in: Reviews in Mineralogy, Vol. 32 (Mineralogical Society of America, Washington, DC, 1995) ch. 5, pp. 121–143.
[11] P.C. Hess, in: Reviews in Mineralogy, Vol. 32 (Mineralogical Society of America, Washington, DC, 1995) ch. 6, pp. 145–190.
[12] G.N. Greaves, S.J. Gurman, C.R.A. Catlow, A.V. Chadwick, S. Houde-Walter, C.M.B. Henderson and B.R. Dobson, Philos. Mag. A64 (1991) 1059.
[13] J. Mahler and A. Sebald, Solid State NMR 5 (1995) 63.
[14] I. Farnan, P.J. Grandinetti, J.H. Baltisberger, J.F. Stebbins, U. Werner, M.A. Eastman and A. Pines, Nature 358 (1992) 31.
[15] R.E. Youngman and J.W. Zwanziger, J. Non-Cryst. Solids 168 (1994) 293.
[16] R.E. Youngman and J.W. Zwanziger, J. Am. Chem. Soc. 117 (1995) 1397.
[17] J.W. Zwanziger, K.K. Olsen and S.L. Tagg, Phys. Rev. B47 (1993) 14618.
[18] M.J. Duer, S.R. Elliot and L.F. Gladden, J. Non-Cryst. Solids 189 (1995) 107.
[19] G. Engelhardt and D. Michel, High-Resolution Solid-State NMR of Silicates and Zeolites (Wiley, Chichester, 1987).
[20] A. Bax, N.M. Szeverenyi and G.E. Maciel, J. Magn. Reson. 55 (1983) 494.
[21] A. Bax, N.M. Szeverenyi and G.E. Maciel, J. Magn. Reson. 52 (1983) 147.
[22] L. Frydman, G.C. Chingas, Y.K. Lee, P.J. Grandinetti, M.A. Eastman, G.A. Barrall and A. Pines, J. Chem. Phys. 97 (1992) 4800.
[23] R. Tycko, G. Dabbagh and P.A. Mirau, J. Magn. Reson. 85 (1989) 265.
[24] J.Z. Hu, D.W. Alderman, C. Ye, R.J. Pugmire and D.M. Grant, J. Magn. Reson. A105 (1993) 82.
[25] P.J. Grandinetti, J.H. Baltisberger, A. Llor, Y.K. Lee, U. Werner, M.A. Eastman and A. Pines, J. Magn. Reson. A103 (1993) 72.
[26] M. Mehring, 'High NMR spectroscopy in solids', in: NMR – Basic Principles and Progress, 2nd Ed., Vol. 11 (Springer, Berlin, 1983).
[27] J.F. Stebbins, S. Sen and I. Farnan, Am. Mineral. 80 (1995) 861.
[28] M.A. Eastman, P.J. Grandinetti, Y.K. Lee and A. Pines, J. Magn. Reson. 98 (1992) 333.
[29] E. Dupree and R.F. Pettifer, Nature 308 (1984) 523.
[30] M.E. Brandriss and J.F. Stebbins, Geochim. Cosmochim. Acta 52 (1988) 2659.
[31] E.D. Lacy, Phys. Chem. Glasses 6 (5) (1965) 171.